NJC

New Journal of Chemistry

A journal for new directions in chemistry

Accepted Manuscript

This article can be cited before page numbers have been issued, to do this please use: A. Belyaev, I. Kolesnikov, A. S. Melnikov, V. V. Gurzhiy, S. P. Tunik and I. O. Koshevoy, *New J. Chem.*, 2019, DOI: 10.1039/C9NJ03426A.

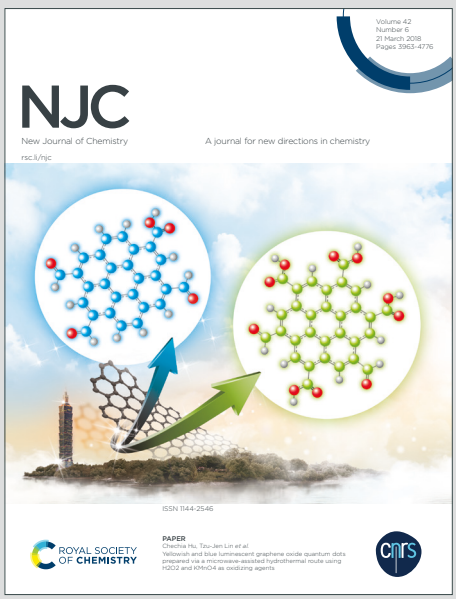

This is an Accepted Manuscript, which has been through the Royal Society of Chemistry peer review process and has been accepted for publication.

Accepted Manuscripts are published online shortly after acceptance, before technical editing, formatting and proof reading. Using this free service, authors can make their results available to the community, in citable form, before we publish the edited article. We will replace this Accepted Manuscript with the edited and formatted Advance Article as soon as it is available.

You can find more information about Accepted Manuscripts in the Information for Authors.

Please note that technical editing may introduce minor changes to the text and/or graphics, which may alter content. The journal's standard Terms & Conditions and the Ethical guidelines still apply. In no event shall the Royal Society of Chemistry be held responsible for any errors or omissions in this Accepted Manuscript or any consequences arising from the use of any information it contains.

View Article Online
DOI: 10.1039/C9NJ03426A

ARTICLE

Solution versus Solid-State Dual Emission of the Au(I)-Alkynyl Diphosphine Complexes via Modification of Polyaromatic Spacers

Received 00th January 20xx,
Accepted 00th January 20xx

DOI: 10.1039/x0xx00000x

Andrey Belyaev,*[a] Ilya Kolesnikov,[b] Alexei S. Melnikov,[c] Vladislav V. Gurzhiy,[d] Sergey P. Tunik,[e] Igor O. Koshevoy*[a]

Single molecule luminophores capable of multiple emissions, are essential for the development of new materials with unconventional photophysical behavior. In this work, a family of the diphosphine ligands PPh_2–PAH–PPh_2 with variable polyaromatic hydrocarbon (PAH) spacer (PAH = 9,10-anthracene **L1**, 1,4-naphthalene **L2**, 2,6-naphthalene **L3**, and their diethynyl congeners **L4**–**L6**) were employed to prepare gold(I) complexes (RC_2Au)PPh_2–PAH–PPh_2(AuC_2R) (**1**–**22**), containing a selection of alkynyl groups. Investigation of their optical properties indicates that compounds with anthracene-based diphosphines (**1**–**4** and **13**–**16**) display only ^{1}IL (ππ*) fluorescence with Φ_{em} up to 93%. The naphthalene and diethynyl-naphthalene diphosphine complexes (**5**–**12** and **17**–**22**), however, demonstrate panchromatic emission in the solid state and in solution featuring well-separated low and high energy signals, which originate from ^{1}IL (ππ*) and ^{3}IL (ππ*) transitions along with certain contribution from metal to ligand and ligand to ligand charge transfers.

Introduction

The nature of the ground and excited states of luminescent molecules primarily determines their photophysical characteristics, such as absorption and emission, the rates of radiative and non-radiative processes and, consequently, the excited state lifetimes. Rational design of the emitting molecular skeleton is expected to provide control over the energies of electronic transitions by manipulating the frontier molecular orbitals. Such target modulation of luminescent properties results in solvatochromism, thermally activated delayed fluorescence, stimuli-responsive behavior, long-lived phosphorescence, panchromatic emission, which are suitable for a number of practical applications including electroluminescent devices, sensors and bioimaging.[1,2]

One approach to novel light emitting materials involves the incorporation of late transition metal atoms (Os^{II}, Re^{I}, Ir^{III}, Pt^{II} and $Au^{I/III}$) into an organic chromophore.[3] In particular, the formation of the σ-bond between carbon skeleton and the gold(I) ion by means of heavy atom effect enhances spin-orbit coupling (SOC) and accelerates the rate of intersystem crossing (ISC, i.e. singlet-triplet transition $S_1 \rightarrow T_1$). This leads to a rapid population of the triplet excited state and further can induce "forbidden" phosphorescence ($T_1 \rightarrow S_0$). However, the reports of pure room temperature fluorescence ($S_1 \rightarrow S_0$) from the molecules containing gold atoms indicate that the presence of this heavy element does not necessarily ensure fast ISC rate, and the nature of the ligands also plays an important role in the excited-state dynamics and deactivation mechanisms.[3a, 4] Conversely, in the case of moderate ISC rate constant, compatible with that of fluorescence relaxation, room temperature fluorescence/phosphorescence dual emission ($S_1+T_1 \rightarrow S_0$) can be observed for this sort of gold compounds. Construction of such emitters remains a challenge due to the need to keep a delicate balance of populating the S_1 and T_1 excited states, but potential benefits of this photophysical phenomenon comprise ratiometric oxygen and pH monitoring,[5] white-light generation,[5b, 6] and fluorescence/phosphorescence lifetime imaging.[7]

Dually emissive gold(I) organometallic species predominantly have low nuclearity and belong to the well-studied LAuX type with linear two-coordinate geometry of the metal center. These complexes are conventionally constructed of isolobal to the proton LAu^+ (L = phosphine or *N*-heterocyclic carbene) cationic fragments,[8] which are complemented by σ-bonded aromatic,[4c, 9] alkynyl,[10] or halide[11] X ligands. Among accessible variations of the constituents, phosphine-alkynyl complexes $(R_3PAu–C\equiv C)_n–R'$ prevail in the family of dual gold(I) luminophores due to facile synthesis and functionalization (Figure 1A). Their photophysical properties are mainly regulated by intraligand transitions localized on the alkynyl ligands, which may contain a wide range of conjugated organic groups. As a representative illustration, simultaneous ligand-centered dual fluorescence (prompt and delayed) and phosphorescence of the conjugated (poly)phenylethylene-

[a] Department of Chemistry, University of Eastern Finland, Joensuu, 80101, Finland.
[b] Center for Optical and Laser materials research, [d] Crystallography Department and [e] Institute of Chemistry, St. Petersburg State University, 198504, St. Petersburg, Russia.
[c] St. Petersburg State Polytechnical University, 195251 St. Petersburg, Russia
* Authors for correspondence
E-mail:
Electronic Supplementary Information (ESI) available: [details of any supplementary information available should be included here]. See DOI: 10.1039/x0xx00000x

View Article Online
DOI: 10.1039/C9NJ04264A

gold(I) phosphine complexes was described by the group of Che.[10a] Another molecular design, which is less common, implies the incorporation of a π-

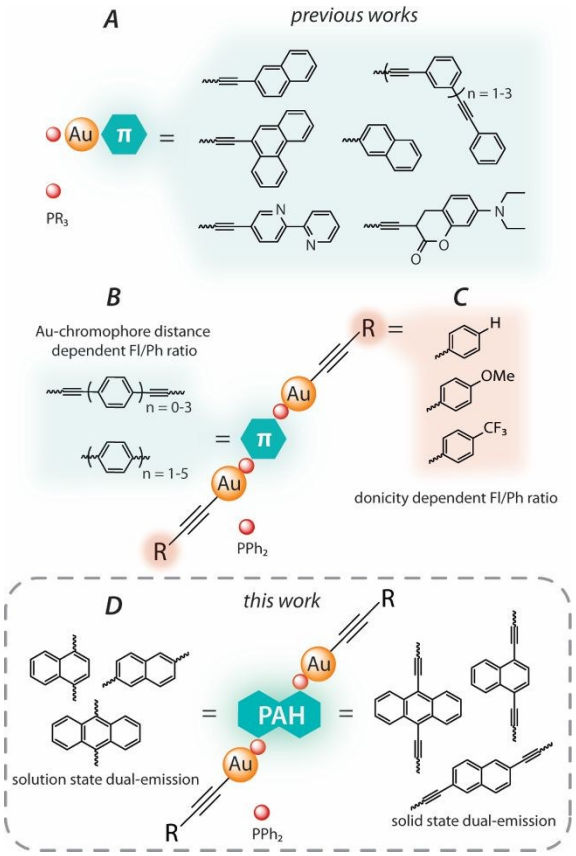

Figure 1. The representative families of previously studied dually emissive phosphine-gold(I) alkynyl complexes (A-C), and the scope of the current work (D).

chromophore spacer into the diphosphine moiety. Utilizing this strategy, we reported a series of dinuclear gold(I) alkynyl complexes based on oligophenylene diphosphine ligands, The rate of ISC for these compounds systematically decreases upon an increase of the effective distance between the heavy gold atom and the center of the chromophore fragment, which allows for fine-tuning the fluorescence/phosphorescence ratio by varying the length of the oligophenylene spacer (Fig. 1B).[6a, 12] Moreover, electronic properties of the ancillary alkynyl substituents (Figure 1C) were shown to affect significantly the rate of ISC process by means of altering the contribution of charge transfer transitions, and therefore influence the probability of singlet vs triplet emission.[13]

In the continuation of our studies, herein, we employ a family of diphosphine ligands based on the polyaromatic spacers (anthracene, naphthalene and their diethynyl derivatives, Fig. 1D). These P-donor modified chromophores were utilized for the preparation of novel gold(I) alkynyl complexes, the luminescence behavior of which was analyzed in solution and in the solid state to correlate with their molecular structures.

Experimental section

General comments. 9,10-bis-(diphenylphosphino)anthracene (**L1**),[4a] $(AuC_2CR)_n$ (R = Ph; 4-C_6H_4-X, X = CF_3, OMe, NH_2, NMe_2, Ph; $C(CH_3)_2OH$; $C_6H_{10}OH$; $C(C_6H_5)_2OH$),[14] diethynylarenes (arene = 9,10-anthracene; 1,4- and 2,6-naphthalene)[15] were synthesized according to the published procedures. Tetrahydrofuran (THF) and diethyl ether were distilled over Na-benzophenone ketyl under a nitrogen atmosphere prior to use. Other reagents and solvents were used as received. The solution on ^{1}H, ^{31}P{^{1}H} and ^{1}H–^{1}H COSY NMR spectra were recorded on a Bruker 400 Avance spectrometer. Mass spectra were determined with a Bruker maXis HD ESI-QTOF instruments in the ESI$^+$ mode. Microanalyses were carried out in the analytical laboratories of the University of Eastern Finland and of Saint-Petersburg State University.

Photophysical measurements. Absorption spectra were recorded using a Lambda 1050 and Shimadzu UV 1800 spectrophotometers; excitation and emission spectra in solution and solid-state were measured on a Fluoromax 4 and Fluorolog 3 spectrofluorimeters. LED (maximum of emission at 265 nm, 340 nm and 390 nm) were used in pulse mode to pump luminescence in fluorescence lifetime measurements (pulse width ~1 ns, repetition rate 100 MHz to 10 kHz). DTL-399QT Laser-export Co. Ltd "(351 nm, 50 mW, pulse width 6 ns repetition rate 0.01-1 kHz), MUM monochromator (LOMO, 1 nm bandwidth), counting head for photons H10682,

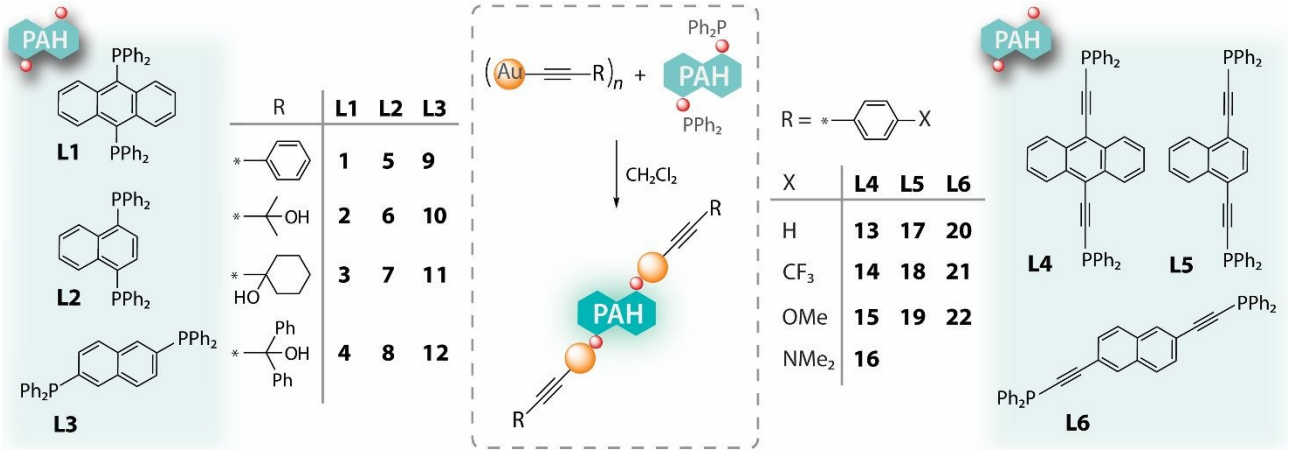

Scheme 1. Polyaromatic phosphine ligands and their gold(I) alkynyl complexes **1–22**

View Article Online
DOI: 10.1039/C9NJ03426A

ARTICLE

(Hamamatsu) and digital time transducer P7887 (FAST ComTec GmbH) were used to measure the phosphorescence lifetime. The emission quantum yield in solution was determined by Vavilov's method[16] using LED (385 nm, continuous mode) and Xenon lamp pumping, with coumarine 102 (Φ_{em} = 0.76) and tryptophan (Φ_{em} = 0.13) as standards. The solutions were carefully degassed by purging Ar for 25 min. The integration sphere Quanta-φ (6-inches) was used to measure the solid state emission quantum yields for the complexes by absolute method.

1,4-Bis-(diphenylphosphino)naphthalene (L2). A 1.6 M solution of *n*-BuLi in hexanes (2.8 mL, 4.5 mmol) was added dropwise to a solution of 1,4-dibromonaphtalene (0.65 g, 2.3 mmol) in diethyl ether (45 ml) at 0 °C. The resulting suspension was stirred at this temperature for 30 min. and then allowed to reach room temperature. It was stirred for an additional hour, then at was treated dropwise with neat PPh_2Cl (1.04 g, 4.7 mmol). Stirring was continued for 3 hours and then the reaction was quenched with a saturated aqueous solution of NH_4Cl (30 ml). Dichloromethane (30 ml) was added to dissolve organic solids. The layers were separated and the aqueous layer was further extracted with dichloromethane (3 x 20 ml). The combined organics were dried over Na_2SO_4, filtered and evaporated. The resulting yellow oil was purified by column chromatography (silica gel, 150 mesh, 2.5 × 15 cm, eluent CH_2Cl_2/hexanes 1:4 v/v) and further recrystallized by slow evaporation of a hexanes/CH_2Cl_2 solution of **L2** at +5 °C to afford colorless crystalline material (0.62 g, 55%). $^{31}P\{^1H\}$ NMR ($CDCl_3$, 298 K; δ): –13.4 (s). ^1H NMR ($CDCl_3$, 298 K; δ): 8.45–8.48 (m, 3,6-H $C_{10}H_6$, 2H), 7.44–7.48 (m, 4,5-H $C_{10}H_6$, 2 H), 7.30–7.36 (m, Ph, 20 H), 6.86–6.87 (m, 1,2-H $C_{10}H_6$, 2H). Anal. Calc. for $C_{34}H_{26}P_2$: C, 82.25; H, 5.28. Found: C 81.98; H 5.34.

2,6-Bis-(diphenylphosphino)naphthalene (L3). Prepared analogously to **L2** from 2,6-dibromonaphtalene (1.00 g, 3.5 mmol). Recrystallization by gas-phase diffusion of diethyl ether into a dichloromethane solution of **L3** at +5 °C afforded colorless crystalline material (1.08 g, 62 %). $^{31}P\{^1H\}$ NMR ($CDCl_3$, 298 K; δ): –4.7 (s). ^1H NMR ($CDCl_3$, 298 K; δ): 7.75 (d, $^3J_{HH}$ 8.4, 3,6-H $C_{10}H_6$, 2H), 7.68 (d, $^3J_{HH}$ 8.4 Hz, 2,5-H $C_{10}H_6$, 2H), 7.4–7.35 (m, Ph and 1,4-H $C_{10}H_6$, 22 H). Anal. Calc. for $C_{34}H_{26}P_2$: C, 82.25; H, 5.28. Found: C, 82.30; H, 5.30.

9,10-Bis-[(diphenylphosphino)ethynyl]anthracene (L4). 9,10-Diethynyl anthracene (0.75 g, 3.3 mmol) was suspended THF (50 ml) and cooled to –78 °C. a 1.6 M solution of *n*-BuLi in hexanes (4.4 ml, 7.0 mmol) was slowly added dropwise. The reaction mixture was warmed to –30 °C within *ca.* 1 h, then cooled to –78 °C again and treated dropwise with neat PPh_2Cl (1.52 g, 6.9 mmol). The reaction mixture was allowed to reach room temperature and was stirred overnight. Then the solvents were evaporated, the solid residue was washed with methanol (3 × 20 ml) and vacuum dried. Crude **L4** was passed through a silica gel (150 mesh, 2.5 × 15 cm, eluent CH_2Cl_2/hexanes 1:1 v/v). Pure sample was obtained by additional treatment of **L4** with activated charcoal in dichloromethane and recrystallization by slow evaporation of a toluene/CH_2Cl_2 solution of **L4** at +5 °C to afford bright yellow needles (1.24 g, 63%). $^{31}P\{^1H\}$ NMR ($CDCl_3$, 298 K; δ): –32.7 (s). ^1H NMR ($CDCl_3$, 298 K; δ): 8.55–8.57 (m, 1,4,5,8-H $C_{14}H_8$, 4H), 7.81–7.85 (m, *ortho*-H Ph, 8 H), 7.57–7.59 (m, 2,3,6,7-H $C_{14}H_8$, 4H), 7.41–7.47 (m, *meta+para*-H Ph, 12H). Anal. Calc. for $C_{42}H_{28}P_2$: C, 84.84; H, 4.75. Found: C, 84.64; H, 4.81.

1,4-Bis-[(diphenylphosphino)ethynyl]naphthalene (L5). Prepared analogously to **L4** from 1,4-diethynylnaphtalene (0.60 g, 3.4 mmol). Recrystallization by gas-phase diffusion of diethyl ether into a dichloromethane solution of **L5** at +5 °C afforded colorless crystalline material (1.34 g, 73%). $^{31}P\{^1H\}$ NMR ($CDCl_3$, 298 K; δ): –33.3 (s). ^1H NMR ($CDCl_3$, 298 K; δ): 8.35-8.37 (m, 2,5-H $C_{10}H_6$, 2H), 7.73-7.78 (m, *ortho*-H Ph and 3,6-H $C_{10}H_6$, 10H), 7.59–7.61 (m, 3,4-H $C_{10}H_6$, 2H), 7.39–7.44 (m, *meta+para*-H Ph, 12H). Anal. Calc. for $C_{38}H_{26}P_2$: C, 83.81; H, 4.81. Found: C, 83.61; H, 4.75.

2,6-Bis-[(diphenylphosphino)ethynyl]naphthalene (L6). Prepared analogously to **L4** from 2,6-diethynylnaphtalene (0.60 g, 3.4 mmol). Recrystallization by slow evaporation of a methanol/CH_2Cl_2 solution of **L6** at +5 °C afforded light yellow crystalline material (1.13 g, 61%). $^{31}P\{^1H\}$ NMR ($CDCl_3$, 298 K; δ): –33.7 (s). ^1H NMR ($CDCl_3$, 298 K; δ): 8.04 (s, 1,4-H $C_{10}H_6$, 2H), 7.78 (d, $^3J_{HH}$ 8.4 Hz, 3,6-H $C_{10}H_6$, 2H), 7.69–7.74 (m, *ortho*-H Ph, 8H), 7.60 (d, $^3J_{HH}$ 8.4 Hz, 2,5-H $C_{10}H_6$, 2H), 7.37–7.42 (m, *meta*, *para*-H Ph, 12H). Anal. Calc. for $C_{38}H_{26}P_2$: C, 83.81; H, 4.81. Found: C, 83.54; H, 4.80.

General procedure for the preparation of complexes 1–22. $(AuC_2R)_n$ (0.3 mmol) was mixed with the corresponding diphosphine (0.16 mmol) in dichloromethane (10 ml). The reaction mixture was stirred for 45 min in the absence of light. The resulting solution was filtered through a Celite pad, vacuum dried and the solid residue was purified by recrystallization. The crystallization and spectroscopic details are given in the ESI.

Result and discussion

Synthesis and characterization

Two families of diphosphine ligands containing polyaromatic hydrocarbon (PAH) backbones (9,10-anthracene (**L1**), 1,4-naphthalene (**L2**), 2,6-naphthalene (**L3**), and their PAH-diethynyl congeners (**L4**–**L6**), Scheme 1) were conventionally

prepared in good yields *via* lithiation of dihalo- or diethynyl PAH precursors and coupling the metalated derivatives with stoichiometric amount of PPh_2Cl.

The dinuclear complexes $(RC_2Au)PPh_2$–*spacer*–$PPh_2(AuC_2R)$ were readily obtained reacting $(AuC_2R)_n$ species with corresponding bidentate ligands under ambient conditions (Scheme 1), analogously to a number of earlier reported congener species.[13-14, 17] The resulting compounds form two series (**1**–**12**) and (**13**–**22**), which are distinguished by the type of stereochemically and electronically different phosphine ligands (tertiary aromatic **L1**–**L3** and ethynyl-aromatic **L4**–**L6**, respectively).

In solution, all the title complexes **1**–**22** were characterized using ESI^+ mass spectrometry and ^1H, ^{31}P NMR spectroscopy. The ESI MS of **1**–**12** (Fig. S1, Supporting Information) show

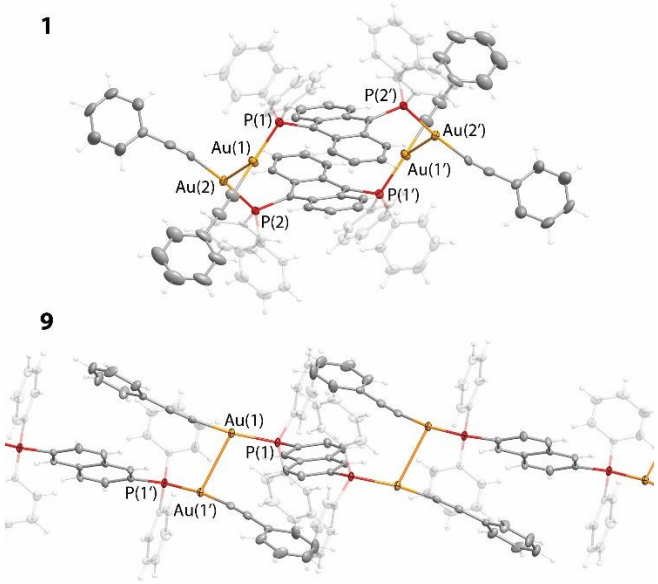

Figure 2. Molecular views of dimer **1** and polymer **9** (thermal ellipsoids are shown at 50% probability).

View Article Online
DOI: 10.1039/C9NJ03426A

the dominating signals of positively charged ion signals generated either by dissociation of alkynyl ligands or by association of the corresponding molecules with Na^+ ions. The $^{31}P\{^1H\}$ NMR spectra of **1**–**22** display singlet resonances with chemical shifts in the ranges 36.3–43.0 ppm (**1**–**12**) and 16.4–17.1 ppm (**13**–**22**), which are typical for the gold(I) compounds containing the related phosphines[13] and are virtually insensitive to the nature of alkynyl ligands. These data indicate that complexes **1**–**22** exist in solution in their molecular forms of idealized symmetry that is additionally supported by the ^1H NMR spectroscopic patterns, completely compatible with molecular arrangements shown in Scheme 1.

Solid-state structures of **1**–**3**, **7**, **9**, **12**, **13** and **19** have been elucidated by the XRD analysis (Figs. 1, 2 and S2); selected structural parameters are summarized in Table S2. Complexes **1** and **9** containing $–C_2Ph$ ligands display intermolecular Au–Au interactions to form a dimeric structure and infinite polymeric

The metal-metal distances in **1** (3.092 Å) and **9** (3.212 Å) are typical for aurophilic bonding frequently encountered in the crystals of gold(I) phosphine compounds.[18]

The Au(I) species with hydroxyaliphatic alkynes (**2**, **3**, **7** and **12**) do not feature metallophilic contacts (Figs. 3 and S2). Alternatively, complexes **2** and **3** with anthracene diphosphine **L1** demonstrate extensive intermolecular O–H···O hydrogen bonding (O···O separations are 2.76–2.88 Å) that evidently affects molecular packing for these species (Figs. S2 and S3). The visible bending of anthracene motif in **1**–**3** is similar to that observed for other gold compounds based on **L1**, and has been tentatively attributed to intramolecular steric hindrance.[4a, 19]

View Article Online
DOI: 10.1039/C9NJ03426A

ARTICLE

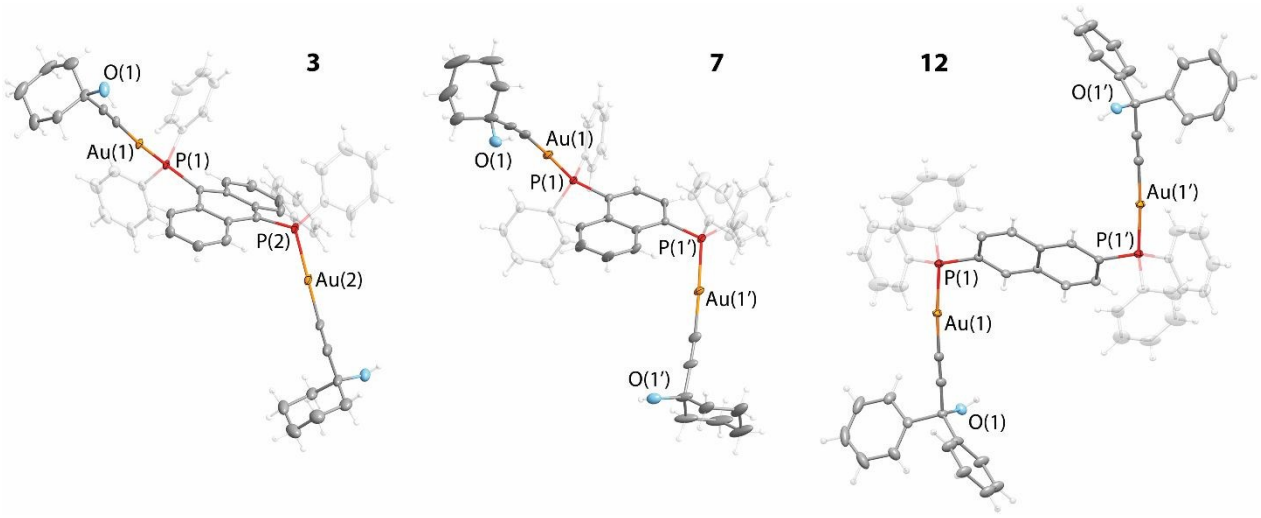

Figure 3. Molecular views of complexes **3**, **7** and **12** (thermal ellipsoids are shown at 50% probability).

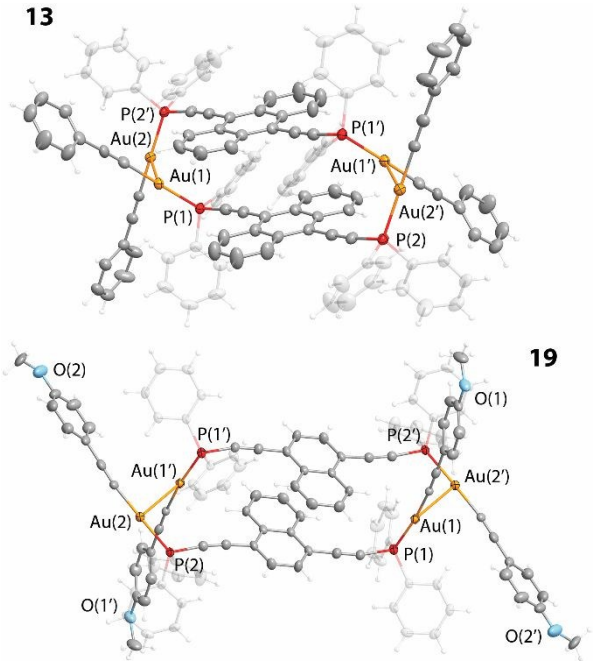

Figure 4. Molecular views of dimers 1**3** and **19** (thermal ellipsoids are shown at 50% probability).

View Article Online
DOI: 10.1039/C9NJ03426A

ARTICLE

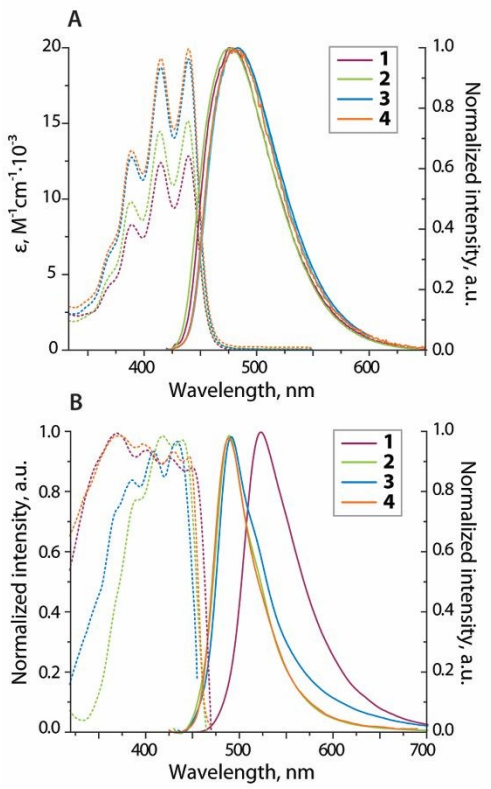

Figure 5. (A) UV-vis absorption (dotted lines) and normalized emission (solid lines) spectra of **1–4** in CH_2Cl_2 (298 K, λ_{ex} = 415 nm); (B) normalized solid-state excitation (dotted lines) and emission (solid lines) spectra of **1–4** (298 K, λ_{ex} = 415 nm).

Photophysical properties

Complexes 1–4. The absorption and emission spectra of **1–4** are shown in Fig. 5, while the corresponding data are given in Table 1. These complexes display similar absorption spectra which are nearly identical to those of the free diphosphine ligand **L1** and its reported gold(I) compounds.[4a, 19b] Analogously to the previous analysis, intense high energy (270 nm) and low energy (370–470 nm) vibronically structured absorption bands can be assigned to the π–π* transitions localized within anthracene rings, though some contribution from σ(Au–P)→π* into the LE absorptions cannot be excluded.[20]

Complexes **1–4** are luminescent in solution at room temperature (Figure 5A). Their emission profiles, small Stokes shift and the lifetimes of ca. 3 ns fit well with fluorescence behavior of cationic complexes $[Au_3(\mathbf{L1})_3]^{3+}$, $[Au_4(\mathbf{L1})_2(\mu\text{-bipy})_2]^{4+}$ $[Au_4(\mathbf{L1})(\text{diethyldithiocarbamate})_3]^{+}$,[4a, 19b, 21] and of the oxide derivative **O=L1**.[22] Thus, the observed emission of **1–4** has mainly an intraphosphine character (^{1}IL) and is virtually independent on the nature of ancillary ligands. The unstructured fluorescence signals for these complexes, which are red shifted in comparison to the parent anthracene, point to some charge transfer contribution into the emissive excited state due to the presence of coordinated PPh_2 groups. The luminescence quantum yields for **1–4** of a few percent only can be attributed to the gold-induced heavy atom effect that facilitates fast ISC and leads to the population of the dark triplet state. Furthermore, larger rates of $S_1 \rightarrow T_1$ transition are known to increase the radiationless internal conversion $S_1 \rightarrow S_0$.[10e]

The emission and excitation characteristics of **2–4** at room temperature in the solid state resemble those measured in solution (Fig. 5B). The emission band maxima are slightly red shifted with respect to the fluid medium, whereas the quantum yield decreases considerably pointing to effective aggregation-caused quenching effect, which often operates for organic luminophores.

In contrast to **2–4**, complex **1** displays ca. 40 nm bathochromic shift of luminescence in the solid state, that is presumably determined by the dimeric structure and π-stacking of the anthracene chromophores, see Fig. 1. These intermolecular interactions apparently raise the ground state energy and decrease the energy gap between the S_0 and S_1 states. For all complexes of this group, the excited state lifetimes fall in the nanosecond domain that confirms the singlet origin of emission.

At 77 K the emission bands of **2–4** exhibit vibronic progressions of ca. 1000-1200 cm^{-1} without a substantial shift of the band center that clearly points to intraligand **L1** origin of fluorescence (Fig. S4A). The broad emission of **1** at 77K suggest that more than one excited state operate upon cooling. This feature evidently crystal packing effect, i.e. the influence of π-stacking and metal-metal interactions, as the spectrum of **1** in frozen solution (CH_2Cl_2) resembles those of **2–4** (Fig. S4B).

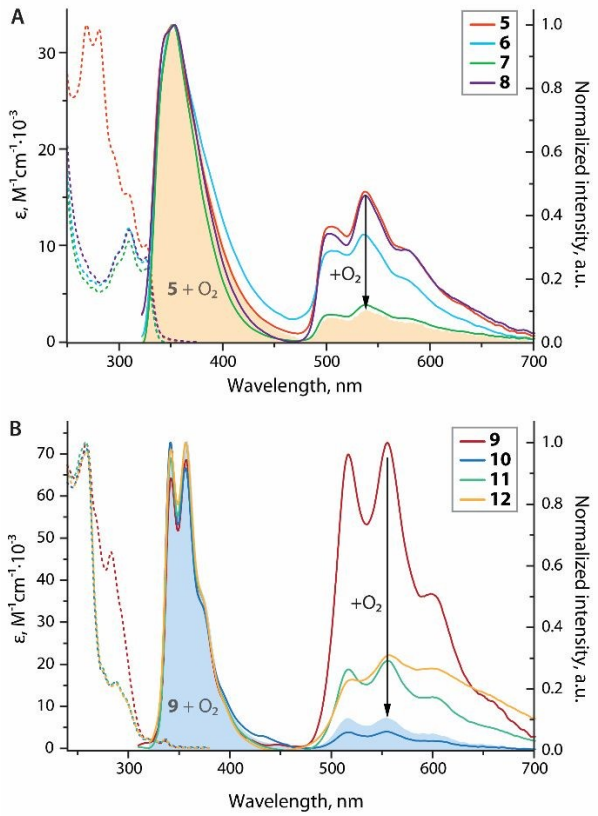

Figure 6. Room temperature UV-vis absorption (dotted lines) and normalized emission (solid lines) spectra of **5–8** (A, λ_{ex} = 310 nm) and **9–12** (B, λ_{ex} = 300 nm) in degassed CH_2Cl_2; color-filled profiles correspond to the spectra of **5** (peach, A) and **9** (blue, B) in aerated solutions.

Table 1. Photophysical properties of complexes **1–4**.

	Solution (CH_2Cl_2, 298 K)				Solid		
	λ_{abs}, nm ($\varepsilon\times10^{-3}$, cm^{-1} M^{-1})	λ_{em}[a], nm	Φ_{em}[b], %	τ_{obs}, ns	λ_{em}[a], nm 298 K	$\lambda_{em.}$[a], nm 77 K	Φ_{em}[c], %
L1	277, 355sh, 374, 396, 419						
1	270 (86), 281 sh (57), 368sh (4), 389 (8), 415 (12), 440 (13)	485	3	2.3	522	~554	<1%
2	271 (63), 367sh (5), 389 (10), 415 (15), 440 (15)	475	4	3	489	467, 490, 506sh	<1%
3	271 (80), 366 (6), 388 (13), 415 (19), 439 (20)	480	5	3	492	464, 488, 522sh	<1%
4	270 (83), 366 (6), 389 (13), 415 (20), 439 (20)	480	4	3.2	489	477, 508, 545sh	<1%

[a] λ_{ex} = 415 nm; [b] measured in degassed solution; [c] in KPF_6 tablet.

Complexes 5–8 and 9–12. Table 2 summarizes photophysical data for the series **5–8** and **9–12**, the relevant solution and solid-state spectra are presented in Figs. 6, S5 and S6. Changing the 9,10-anthracene backbone in the diphosphine ligand for the 1,4-naphthalene (**L2**-based complexes **5–8**) or 2,6-naphthalene (**L3**-based complexes **9–12**) leads to the essential variation of the photophysical behavior of the resulting gold(I) alkynyl complexes.

In solution, complexes **5–8** and **9–12** display dual emission, which comprises the HE band centered at ca. 350 nm and a structured LE band with wavelength above 500 nm. Vibronic progression of the LE band of ca. 1300–1500 cm^{-1} is normal for the gold-bound aromatic chromophores[9b, 23] and therefore points to a ligand centered (**L2** naphthalene backbone) nature of this emission. A large Stokes shift together with oxygen quenching of LE signal, as depicted in Fig. 5, are indicative of the triplet origin of this band (phosphorescence), while the HE one, which also shows vibronic structure for **9–12** series (Δν ~1200 cm^{-1}) and is not sensitive to the presence of molecular oxygen, is associated intraligand fluorescence of **L2** (**5–8**) and **L3** (**9–12**) diphosphines, visibly perturbed for **5–8** by the $-PPh_2AuR$ motifs. Unfortunately, low intensity of luminescence (Φ_{em} < 0.1%) did not allow to determine accurately the lifetimes of singlet and triplet excited states to confirm their multiplicities.

View Article Online
DOI: 10.1039/C9NJ03426A

ARTICLE

Table 2. Photophysical properties of complexes **5–12**.

	Solution (CH_2Cl_2, 298 K)		Solid			
	λ_{abs}, nm ($\varepsilon \times 10^{-3}$, $cm^{-1}\ M^{-1}$)	λ_{em}[a], nm	λ_{em}[b], nm 298 K	$\lambda_{em.}$[b], nm 77 K	τ_{av}[c], μs	Φ_{em}[d], %
L2	274 (6), 332 (6)					
5	268 (32.5), 280 (32), 296 sh (19), 310 (15), 326 (10)	350, 503, 538, 580	506, 536, 582	511, 524, 540, 590sh	13.2	2
6	275 (7), 297 (10), 310 (11), 326 (8.5)	351, 501, 536, 583	497, 509sh, 536, 580, 632	497, 510, 535, 549, 576	2.4	<1%
7	274 (6.5), 297 (9.5), 310 (11), 326 (7)	351, 501, 536, 586	510, 536, 580sh	516, 533, 550	2.1	<1%
8	273 (7), 297 (10), 310 (11), 326 (8.5)	352, 502, 540, 582	498, 510, 536, 578, 630	514, 523sh, 553, 600	86.3	<1%
L3	270 (17), 310 9)					
9	258 (72), 283 (46), 293 (33), 310 (15), 320 (2.3), 336 (2)	341, 356, 516, 555, 600	478, 520sh, 557, 605sh	488, 524, 555, 605sh	225.9	<1%
10	258 (72), 275 (19), 288 (16), 298 (11), 320 (2.3), 336 (2)	340, 356, 373, 514, 555, 604	475, 521, 554, 605, 664sh	486sh, 519, 552, 600sh	205.9	2
11	258 (72), 275 (19), 288 (16), 298 (11), 320 (2.3), 336 (2)	341, 356, 514, 555, 603	513, 551, 597, 654	507, 546, 592, 647	1694.4	5
12	258 (72), 275 (19), 288 (16), 298 (11), 320 (2.3), 336 (2)	342, 357, 517, 557, 603	509, 548, 593, 648	504, 515, 543, 589, 645	1407.4	7

[a] λ_{ex} = 310 nm for **5–8** and 300 nm for **9–12**; [b] λ_{ex} = 330 nm; [c] average emission lifetimes for the two-exponential decay determined using the equation $\tau_{av} = (A_1\tau_1^2 + A_2\tau_2^2)/(A_1\tau_1 + A_2\tau_2)$, where A_i is the weight of the i-exponent; [d] in KPF_6 tablet.

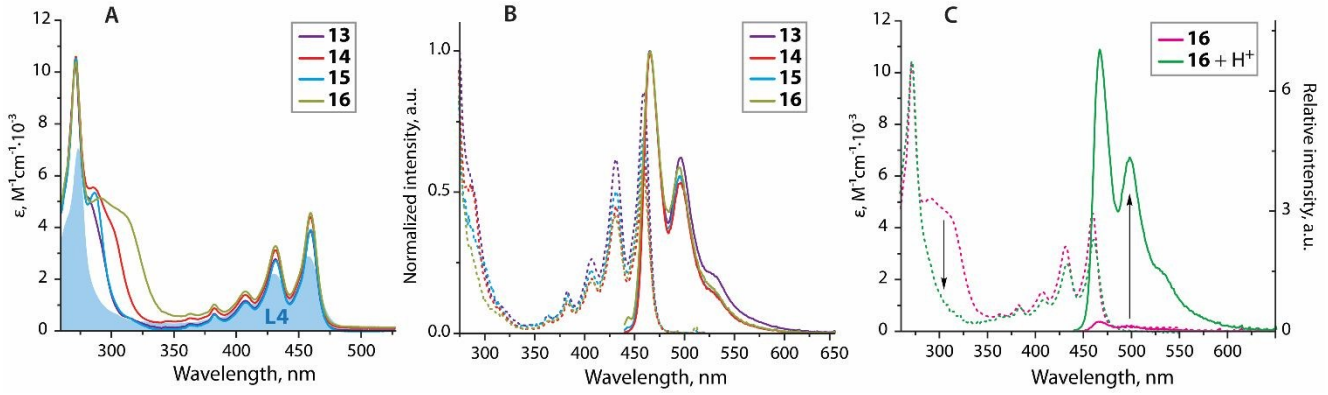

Figure 7. (A) UV-vis absorption spectra of **13–16**, color-filled profile corresponds to **L4** (CH_2Cl_2, 298 K); (B) normalized excitation (dotted lines) and emission (solid lines) spectra of **13–16** (CH_2Cl_2, 298 K); (C) changes of absorption and emission spectra of **16** upon protonation by CF_3COOH.

View Article Online
DOI: 10.1039/C9NJ03426A

Table 3. Photophysical properties of complexes **13–16**.

	Solution (CH_2Cl_2, 298 K)				Solid			
	λ_{abs}, nm ($\varepsilon\times10^{-3}$, cm^{-1} M^{-1})	λ_{em}[a], nm	Φ_{em}, %	τ_{obs}, ns	λ_{em}[b], nm 298 K	λ_{em}[b], nm 77 K	Φ_{em}, %	τ_{obs}, ns
L4	273, 381, 406, 430, 458	-	-	-	-		-	-
13	270 (103), 363 (3), 382 (7), 407 (12), 431 (28), 460 (39)	465, 495, 530	87	4.2	541	530, 575sh	4	3.8
14	271 (106), 286 (53), 363 (2), 382 (7), 407 (11), 431 (27), 460 (39)	465, 495, 530	93	4.4	535	516, 555	5	5.5
15	270 (106), 286 sh (56), 363 (5), 382 (9), 407 (14), 431 (31), 460 (44)	465, 495, 530	2	4.2	541	525, 562	1	11.8
16	271 (104), 289 sh (53), 311 (46), 363 (7), 382 (10), 407 (15), 431 (33), 460 (46)	465, 495, 530	1	4.0	-		-	-
16H^{+c}	271 (105), 384 (9), 408 (12), 433 (26), 461 (36)	465, 495, 530	39	4.7	-		-	-

[a] λ_{ex} = 430 nm; [b] λ_{ex} = 350 nm; [c] **16** in the presence of 0.1 M CF_3COOH in CH_2Cl_2.

The positions of the emission maxima are very similar within each group of complexes and the spectra are only different in relative intensities of HE fluorescence and LE phosphorescence bands (Figure 6). The invariance of the emission energies and thus of the lowest lying excited states (S_1 and T_1) is in line with poor involvement of the alkynyl ligands in their composition. However, as we have shown earlier, the ancillary $–C_2R$ groups are capable to affect the rate of intersystem crossing $S_1 \rightarrow T_n$ ($n \geq 1$), altering the contribution of MLCT/L´LCT transitions [13] The non-innocent role of alkynyl ligands in populating the T_1 state is also seen for **5–8** and **9–12** (see the excitation spectra in Fig. S5), in which phenylakynyl complexes **5** and **9** show the largest phosphorescence *vs.* fluorescence ratio within each series.

It is worth comparing the photophysical performance of **5–12** with that of the structurally related complexes of isomeric 1,8-bis(diphenylphosphino)naphthalene studied by Yam.[20] In the latter case, the close disposition of the phosphorus substituents on the naphthalene backbone results in a virtually complete suppression of the singlet emission in solution to give phosphorescence in a red region (λ_{em} > 700 nm) and microsecond lifetimes. These emission characteristics drastically differ from those of **5–12** and illustrate the effect of substitutional isomerism of the diphosphines (i.e. 1,4-naphthalene (**L2**), 2,6-naphthalene (**L3**) and 1,8-naphthalene[20]) in the modulation of the lowest lying excited state.

In solid state, luminescence efficiency of **5–8** and **9–12** series is enhanced compared to that in solution, the quantum yields fall in the range of 1–7% (Table 2). All complexes of these groups both at room temperature and at 77 K display structured LE bands with line shapes, which resemble the profiles of the phosphorescence profiles revealed in solution (Fig. S6). The long lifetimes (2.1–86.3 μs for **5–8** and 206–1694 μs for **9–12**) imply that only triplet emission retains in solid.

Complexes 13–16, 17–19 and 20–22. It has been shown earlier that gold complexes constructed of the diphosphines with diethynyl-phenylene spacers, $Ph_2P–C_2–(C_6H_4)_n–C_2–PPh_2$, often exhibit higher quantum efficiencies than their counterparts composed of the ligands with phenylene backbones $Ph_2P–(C_6H_4)_n–PPh_2$.[6a, 24] Therefore, low emission intensities of compounds **1–12**, which contain PPh_2-functionalized PAH moieties, prompted us to investigate photophysical characteristics of congener complexes **13–22** bearing ethynyl-modified ligands **L4–L6**. Simultaneously, within these series we have systematically altered the electronic properties of auxiliary phenylacetylene groups $–C_2C_6H_4–X$ (X = CF_3, H, OMe, NMe_2) to inspect their influence on the optical behavior of intra-phosphine PAH chromophores.

Complexes $(AuC_2C_6H_4X)_2$**L4** (X = H, **13**; CF_3, **14**; OMe, **15**; NMe_2, **16**) with diethynyl-anthracene phosphine show absorptions spectra, which are mainly derived from that of the free ligand

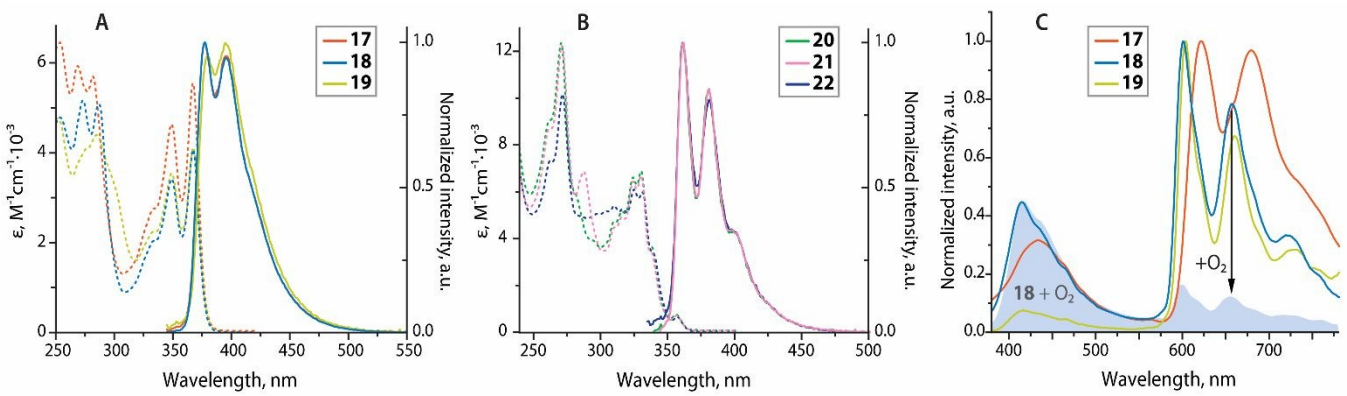

Figure 8. Room temperature UV-vis absorption (dotted lines) and normalized emission (solid lines) spectra of **17–19** (A) and **20–22** (B) in degassed CH_2Cl_2; (C) normalized solid-state emission spectra of **17–19** under an Ar atmosphere, color-filled profile corresponds to the spectra of **18** on air.

View Article Online
DOI: 10.1039/C9NJ03426A

Table 4. Photophysical properties of complexes **17–22**.

	Solution (CH_2Cl_2, 298 K)				Solid				
	λ_{abs}, nm ($\varepsilon\times10^{-3}$, cm^{-1} M^{-1})	λ_{em}[a], nm	Φ_{em}, %	τ_{obs}, ns	λ_{em}[a], nm 298 K	λ_{em}[a], nm 77 K	Φ_{em}[b], %	τ_f[c], ns	$\tau_{ph(av)}$[d], μs
L5	250 (39), 327 (14), 348 (25), 368 (28)	-	-	-	-		-	-	
17	253 (65), 268 (60), 281 (57), 332 (28), 348 (47), 367 (55)	377, 397	8	0.5	432, 622, 680	454, 472 sh, 628, 689, 758	3	5.3	249.4
18	254 (47), 273 (52), 286 (51), 333 (21), 348 (34), 367 (41)	377, 397	24	0.6	414, 601, 658, 723	414, 438, 614, 666, 733	2	3.7	54.8
19	253 (48), 272sh (41), 284 (44), 332 (23), 348 (36), 367 (41)	380, 396	1	1.6	414, 603, 660, 727	414, 438, 602, 620, 664, 730	3	4.0	85.1
L6	267 (39), 328 (23), 342 (25)								
20	261 (90), 271 (123), 284sh (55), 296 (39), 310 (48), 316 (51), 324 (67), 331 (69), 338 (37), 357 (8)	361, 380, 400	4	1.1	400, 551	550, 562, 600, 621, 650	<1%	3.4	5.9
21	262 (87), 272 (121), 286 (69), 310 (44), 316 (49), 324 (64), 331 (66), 338 (37), 357 (8)	361, 380, 400	11	1.2	390, 542, 590, 647	385, 544, 556, 593, 644	1	2.9	91.6
22	262 (74), 272 (101), 286 (50), 298 (50), 305 (52), 310 (54), 316 (52), 324 (61), 331 (60), 338 (37), 357 (8)	361, 380, 400	<1%	2.7	410, 540, 590	536, 550, 587, 631	<1%	3.7	10.6

[a] λ_{ex} = 330 nm; [b] total quantum yield measured on air at 298 K; [c] for HE fluorescence band at 298 K; [d] for LE phosphorescence band at 298 K, average emission lifetimes for the two-exponential decay determined using the equation $\tau_{av} = (A_1\tau_1^2 + A_2\tau_2^2)/(A_1\tau_1 + A_2\tau_2)$, where A_i is the weight of the i-exponent.

L4 (Table 3 and Fig. 7). In addition to the absorption bands of the phosphine, complexes **13–16** display moderately intense absorption shoulders in the range 286–311 nm, which can be attributed to C≡CR intraligand transitions. The emission profiles for **13–16** are nearly the same irrespectively of the C≡CR ligand and also match the spectra of $(PR_3Au)_2$(9,10-diethynylanthracene) complexes meaning that the PAH core of **L4** determines the luminescence properties.[20, 25] The structured signals, high intensity (Φ_{em} = 87% and 93% for **13** and **14**) and nanosecond lifetimes prove the ^{1}IL (anthracene) nature of the excited state. The excitation spectra of **13–16** (Fig. 7B) are essentially alike to the absorption spectrum of **L4**, meaning that LL´ (π C_2R → π* **L4**)/ML (Au d_π → π* **L4**) charge transfers play a minor role for the lowest lying excited state S_1. Despite the modulation of electron donating ability of –$C_2C_6H_4X$ alkynyl ligands does not change the shape **14** (X = CF_3) is the most intense fluorophore among the studied compounds (Φ_{em} = 93%), gradual increasing the basicity of X substituents leads to a drastic drop of the quantum yield for **16** (X = NMe_2, Φ_{em} = 1%). A similar trend was observed for Au(I) complexes with oligophenylene π-chromophores, for which, however, changing X = CF_3 for OMe primarily enhances phosphorescence *vs* fluorescence emission.[13] To gain additional experimental proof that alkynyl ligands can govern the radiationless decay pathways, the photophysics of complex **16** has been studied in the presence of trifluoroacetic acid. Indeed, protonation of the NMe_2 group results in ca. 35-fold increase of luminescence intensity (Table 3 and Figure 7C) and disappearance of ~300 nm absorption band assigned to $C_2C_6H_4NMe_2$ localized transitions. The latter evidently shifts to higher energies due to stabilization of the alkynyl-aniline π orbitals caused by switching the electron-rich NMe_2 function to electron deficient NMe_2H^+ ammonium derivative.[26]

The solid-state emissions of complexes **13–15** are substantially red shifted (ca. 75 nm) with respect to their solution spectra (Figure S7), **16** is not luminescent. Additionally, the loss of vibronic structure, dramatically lower intensity (Φ_{em} up to 5% for **14**) and short emission lifetimes of several nanoseconds evidence fluorescence, probably arising from intermolecular charge transfer between the PAH chromophores, which tend to aggregate in the solid state.

The photophysical data for the series **17–19** and **20–22** with 1,4- and 2,6-diethynylnaphthalene emitting centers, respectively, are listed in Table 4. In solution both groups of complexes reveal singlet emission HE signals in deep blue to violet region with maximum quantum yields reached by CF_3-substituted alkynyl species **18** (Φ_{em} = 24%) and **21** (Φ_{em} = 11%). Analogously to the anthracene-based family **13–16** described above, the naphthalene compounds **17–22** manifest a steep dependence of fluorescence intensity on the electron richness of the alkynyl ligands, which do not affect the energies of the bands (Figure 8).

In the solid state, complexes **17–22** behave differently than in solution and display two emission bands, which are particularly pronounced for CF_3-containing compounds **18** and **21** (Figures 8C and S8, S9). The broadened unresolved HE signals, which have the lifetimes of few nanoseconds, are red shifted for ca. 30 nm with respect to the corresponding

View Article Online
DOI: 10.1039/C9NJ03426A

fluorescence bands in solution. The intensity of long-lived LE emissions (λ_{em} > 600 nm for **17–19** and > 540 for **20–22**) is readily reduced on air, the extent of quenching is supposedly dependent on the morphology of the solid sample and is facilitate by its intrinsic porosity.[13] Notably, the Commission Internationale de l'Eclairage (CIE) coordinates of the compound **21** in the solid state (Table S3) correspond to nearly pure white color (0.32, 0.32). The fluorescence *vs* phosphorescence ratio for **17–19** at 298 K can be correlated with donicity of alkynyl ligands, the increase of which favors transition to the T_1 state, and therefore explained in terms of variable MLCT/L´LCT contributions.[13] However, the triad **20–22** does not obey the given trend (Figure S9) that testifies to the presence of subtle effects, which operate in solid phase and have fine influence on the optical characteristics.

It is pertinent to remark the discrepancy in emission behavior for **17**, **20** and of their aryl relatives **5** and **9** bearing same phenyl alkynyl ligands. The latter complexes are dually emissive in solution, but in the solid state demonstrate pure phosphorescence. In a simplified approach, the difference in inducing triplet luminescence in **17**, **20** *vs* **5**, **9** stems from the nature of coordinating group, which links the chromophore PAH center to the gold ion and therefore determines the electronic communication and the distance between them. The smaller separation PAH···Au in **5**, **9** presumably facilitates spin-orbit coupling primarily *via* heavy atom effect and rises the rate of intersystem crossing $S_1 \rightarrow T_n$ so that phosphorescence starts to compete with fluorescence in fluid medium and prevails in solid samples. In line with this rationalization, the direct bonding of naphthalene to $\{AuPR_3\}$ fragments almost completely suppresses singlet emission already in solution.[4c] In the case of **17–22** the additional ethynyl spacers of the diphosphine backbones increase both the PAH···Au gap and fluorescence quantum efficiency, but prevent triplet emission in solution due to poor ISC. On the other hand, for these compounds dual luminescence is attained in the solid state that provides a route to molecular materials for panchromatic light generation.

Conclusions

In this work, we have synthesized a series of luminescent dinuclear gold(I) alkynyl complexes constructed of phosphine-functionalized polyaromatic (PAH) chromophores. Systematic alteration of PAH moieties, the position and electronic features of P-donor connectivities reveal an essential influence on the optical behavior of the metal compounds. The anthracene-based gold(I) complexes **1–4** and **13–16** apparently demonstrate intraligand fluorescence localized on the diphosphine backbone with negligible contribution of the alkynyl and metal *d* orbitals into the emissive excited state. An extension of the PAH spacer (anthracene → diethynylanthracene) appears to be an efficient tool for increasing quantum yield in solution; compounds **1–4** show Φ_{em} up to 5%, whereas for **13–16** Φ_{em} reaches 93%. Increasing the basicity of substituents X in alkynyl ligands $-C_2C_6H_4X$ leads to a drastic drop of the emission intensity (X = CF_3, Φ_{em} = 93% → X = NMe_2, , Φ_{em} = 1%) complexes **13–16**. The replacement of the anthracene motif for the naphthalene core produces distinct dual emission in solution for **L2** and **L3**-based complexes **5–12**. Their luminescence profiles comprise the high-energy fluorescence band centered at ca. 350 nm and vibronically structured phosphorescence signal with the wavelength maxima above 500 nm. In the solid state, the fluorescence signals for these species are completely suppressed and only triplet emission is observed. In contrast to **5–12**, their ethynyl-phosphine congeners **17–22** (**L4** and **L5**-based compounds) in solution exhibit only structured HE fluorescence, as manifested by nanosecond lifetimes of the excited state, with maximum quantum yields attained for **18** (Φ_{em} = 24%) and **21** (Φ_{em} = 11%) with CF_3-substituted alkynyl groups. However, as solid powders complexes **17–22** are dually luminescent at room temperature. This effect is tentatively ascribed to the influence of ethynyl fragments between the phosphorus atoms and the π-spacers, which increase the PAH···Au distance and consequently diminishes spin-orbit coupling, resulting in radiative relaxation of both S_1 and T_1 states only in the solid state.

Conflicts of interest

There are no conflicts to declare.

Acknowledgements

Financial support from the Academy of Finland (grant 317903, I.O.K.) and Russian Science Foundation (spectral characterization and photophysical studies, grant 19-13-00132, S.P.T.) is gratefully acknowledged. The work was performed using the equipment of the Analytical Centre for Nano- and Biotechnologies (Peter the Great St Petersburg Polytechnic University with financial support from the Ministry of Education and Science of Russian Federation); Centers for Magnetic Resonance, for Optical and Laser Materials Research, for Chemical Analysis and Materials Research, Research Park of St. Petersburg State University.

References

1. (a) C. Reichardt, *Chem. Rev.*, 1994, **94**, 2319-2358; (b) N. Siraj, B. El-Zahab, S. Hamdan, T. E. Karam, L. H. Haber, M. Li, S. O. Fakayode, S. Das, B. Valle, R. M. Strongin, G. Patonay, H. O. Sintim, G. A. Baker, A. Powe, M. Lowry, J. O. Karolin, C. D. Geddes, I. M. Warner, *Analytical Chemistry*, 2016, **88**, 170-202.
2. (a) X.-K. Chen, D. Kim, J.-L. Brédas, *Acc. Chem. Res.*, 2018, **51**, 2215-2224; (b) S.-C. Lee, J. Heo, H. C. Woo, J.-A. Lee, Y. H. Seo, C.-L. Lee, S. Kim, O. P. Kwon, *Chem. Eur. J.*, 2018, **24**, 13706-13718; (c) L. Wang, M. S. Frei, A. Salim, K. Johnsson, *J. Am. Chem. Soc.*, 2019, **141**, 2770-2781.
3. (a) Y. Y. Chia, M. G. Tay, *Dalton Trans.*, 2014, **43**, 13159–13168; (b) H. Xu, R. Chen, Q. Sun, W. Lai, Q. Su, W. Huang, X. Liu, *Chem. Soc. Rev.*, 2014, **43**, 3259-3302; (c) F. N. Castellano, *Acc. Chem. Res.*, 2015, **48**, 828–839; (d) V. W.-W. Yam, V. K.-M. Au, S. Y.-L. Leung, *Chem. Rev.*, 2015, **115**, 7589–7728.
4. (a) J. H. K. Yip, J. Prabhavathy, *Angew. Chem. Int. Ed.*, 2001, **40**, 2159-2162; (b) V. W.-W. Yam, K.-L. Cheung, S.-K. Yip, N. Zhu,

DOI: 10.1039/C9NJ03426A

Photochem. Photobiol. Sci., 2005, **4**, 149-153; (c) L. Gao, M. A. Peay, D. V. Partyka, J. B. Updegraff, T. S. Teets, A. J. Esswein, M. Zeller, A. D. Hunter, T. G. Gray, *Organometallics*, 2009, **28**, 5669–5681; (d) M.-H. Nguyen, J. H. K. Yip, *Organometallics*, 2010, **29**, 2422–2429; (e) L. Gao, D. S. Niedzwiecki, N. Deligonul, M. Zeller, A. D. Hunter, T. G. Gray, *Chem. Eur. J.*, 2012, **18**, 6316-6327; (f) S. Goswami, R. W. Winkel, K. S. Schanze, *Inorg. Chem.*, 2015, **54**, 10007−10014; (g) A. M. Christianson, F. P. Gabbaï, *Inorg. Chem.*, 2016, **55**, 5828−5835; (h) J. R. Shakirova, O. A. Tomashenko, E. V. Grachova, G. L. Starova, V. V. Sizov, A. F. Khlebnikov, S. P. Tunik, *Eur. J. Inorg. Chem.*, 2017, **2017**, 4180-4186; (i) A. Gutiérrez-Blanco, V. Fernández-Moreira, M. C. Gimeno, E. Peris, M. Poyatos, *Organometallics*, 2018, **37**, 1795-1800.

5. (a) J. C. Lima, L. Rodriguez, *Chem. Soc. Rev.*, 2011, **40**, 5442–5456; (b) Y. Liu, H. Guo, J. Zhao, *Chem. Commun.*, 2011, **47**, 11471–11473; (c) T. Yoshihara, Y. Yamaguchi, M. Hosaka, T. Takeuchi, S. Tobita, *Angew. Chem. Int. Ed.*, 2012, **51**, 4148-4151; (d) T. Yoshihara, Y. Yamaguchi, M. Hosaka, T. Takeuchi, S. Tobita, *Angew. Chem. Int. Ed.*, 2012, **51**, 4148–4151; (e) P. W. Zach, S. A. Freunberger, I. Klimant, S. M. Borisov, *ACS Appl. Mater. Interfaces*, 2017, **9**, 38008-38023.
6. (a) Y.-C. Chang, K.-C. Tang, H.-A. Pan, S.-H. Liu, I. O. Koshevoy, A. J. Karttunen, W.-Y. Hung, M.-H. Cheng, P.-T. Chou, *J. Phys. Chem. C*, 2013, **117**, 9623–9632; (b) M. Bachmann, O. Blacque, K. Venkatesan, *Chem. Eur. J.*, 2017, **23**, 9451–9456; (c) M. Pan, W.-M. Liao, S.-Y. Yin, S.-S. Sun, C.-Y. Su, *Chem. Rev.*, 2018, **118**, 8889-8935.
7. (a) H. Shi, H. Sun, H. Yang, S. Liu, G. Jenkins, W. Feng, F. Li, Q. Zhao, B. Liu, W. Huang, *Adv. Funct. Mater.*, 2013, **23**, 3268-3276; (b) Q. Zhao, X. Zhou, T. Cao, K. Y. Zhang, L. Yang, S. Liu, H. Liang, H. Yang, F. Li, W. Huang, *Chem. Sci.*, 2015, **6**, 1825–1831; (c) F. Liu, J. Wen, S.-S. Chen, S. Sun, *Chem. Commun.*, 2018, **54**, 1371-1374.
8. H. G. Raubenheimer, H. Schmidbaur, *Organometallics*, 2012, **31**, 2507-2522.
9. (a) W. Y. Heng, J. Hu, J. H. K. Yip, *Organometallics*, 2007, **26**, 6760–6768; (b) D. V. Partyka, T. S. Teets, M. Zeller, J. B. Updegraff, A. D. Hunter, T. G. Gray, *Chem. Eur. J.*, 2012, **18**, 2100–2112.
10. (a) W. Lu, W.-M. Kwok, C. Ma, C. T.-L. Chan, M.-X. Zhu, C.-M. Che, *J. Am. Chem. Soc.*, 2011, **133**, 14120–14135; (b) J. Gil-Rubio, V. Cámara, D. Bautista, J. Vicente, *Organometallics*, 2012, **31**, 5414-5426; (c) K. T. Chan, G. S. M. Tong, W.-P. To, C. Yang, L. Du, D. L. Phillips, C.-M. Che, *Chem. Sci.*, 2017, **8**, 2352–2364; (d) M. Ferrer, L. Giménez, A. Gutiérrez, J. C. Lima, M. Martínez, L. Rodríguez, A. Martín, R. Puttreddy, K. Rissanen, *Dalton Trans.*, 2017, **46**, 13920-13934; (e) E. Aguiló, A. J. Moro, M. Outis, J. Pina, D. Sarmento, J. S. Seixas de Melo, L. Rodríguez, J. C. Lima, *Inorg. Chem.*, 2018, **57**, 13423-13430; (f) S. Wan, W. Lu, *Angew. Chem. Int. Ed.*, 2017, **56**, 1784-1788; (g) E. C. Constable, C. E. Housecroft, M. K. Kocik, M. Neuburger, S. Schaffner, J. A. Zampese, *Eur. J. Inorg. Chem.*, 2009, **2009**, 4710-4717; (h) X.-L. Li, K.-J. Zhang, J.-J. Li, X.-X. Cheng, Z.-N. Chen, *Eur. J. Inorg. Chem.*, 2010, **2010**, 3449-3457.
11. (a) T. L. Stott, M. O. Wolf, B. O. Patrick, *Inorg. Chem.*, 2005, **44**, 620-627; (b) Z. Chen, G. Liu, R. Wang, S. Pu, *RSC Adv.*, 2017, **7**, 15112-15115.
12. I. O. Koshevoy, C.-L. Lin, C.-C. Hsieh, A. J. Karttunen, M. Haukka, T. A. Pakkanen, P.-T. Chou, *Dalton Trans.*, 2012, **41**, 937-945.
13. I. Kondrasenko, K.-y. Chung, Y.-T. Chen, J. Koivistoinen, E. V. Grachova, A. J. Karttunen, P.-T. Chou, Igor O. Koshevoy, *J. Phys. Chem. C*, 2016, **120**, 12196−12206.
14. (a) G. E. Coates, C. Parkin, *J. Chem. Soc.*, 1962, 3220-3226; (b) I. O. Koshevoy, Y.-C. Chang, A. J. Karttunen, S. I. Selivanov, J. Jänis, M. Haukka, T. A. Pakkanen, S. P. Tunik, P.-T. Chou, *Inorg. Chem.*, 2012, **51**, 7392−7403.
15. Y.-P. Ou, C. Jiang, D. Wu, J. Xia, J. Yin, S. Jin, G.-A. Yu, S. H. Liu, *Organometallics*, 2010, **30**, 5763–5770.
16. J. N. Demas, G. A. Crosby, *J. Phys. Chem.*, 1971, **75**, 991-1024.
17. (a) V. W.-W. Yam, S. W.-K. Choi, K.-K. Cheung, *Organometallics*, 1996, **15**, 1734-1739; (b) M. Ferrer, A. Gutiérrez, L. Rodríguez, O. Rossell, J. C. Lima, M. Font-Bardia, X. Solans, *Eur. J. Inorg. Chem*, 2008, 2899–2909.
18. (a) E. R. T. Tiekink, J.-G. Kang, *Coord. Chem. Rev.*, 2009, **253**, 1627–1648; (b) H. Schmidbaur, A. Schier, *Chem. Soc. Rev.*, 2012, **41**, 370-412.
19. (a) K. Zhang, J. Prabhavathy, J. H. K. Yip, L. L. Koh, G. K. Tan, J. J. Vittal, *J. Am. Chem. Soc.*, 2003, **125**, 8452-8453; (b) R. Lin, J. H. K. Yip, K. Zhang, L. L. Koh, K.-Y. Wong, H. K. Piu, *J. Am. Chem. Soc.*, 2004, **126**, 15852-15869.
20. V. W.-W. Yam, S. W.-K. Choi, *J. Chem. Soc., Dalton Trans.*, 1996, 4227-4232.
21. J. Li, X.-F. Zhu, L.-Y. Zhang, Z.-N. Chen, *RSC Adv.*, 2015, **5**, 34992-34998.
22. (a) Z. Fei, N. Kocher, C. J. Mohrschladt, H. Ihmels, D. Stalke, *Angew. Chem. Int. Ed.*, 2003, **42**, 783-787; (b) Y. Zhao, L. Duan, X. Zhang, D. Zhang, J. Qiao, G. Dong, L. Wang, Y. Qiu, *RSC Adv.*, 2013, **3**, 21453-21460.
23. L. Gao, D. V. Partyka, J. B. I. Updegraff, N. Deligonul, T. G. Gray, *Eur. J. Inorg. Chem*, 2009, 2711–2719.
24. V. F. Moreira, J. Cámara, E. S. Smirnova, I. O. Koshevoy, A. Laguna, S. P. Tunik, M. C. Blanco, M. C. Gimeno, *Organometallics*, 2016, **35**, 1141−1150.
25. V. Mishra, A. Raghuvanshi, A. K. Saini, S. M. Mobin, *J. Organomet. Chem.*, 2016, **813**, 103-109.
26. I. O. Koshevoy, A. J. Karttunen, S. P. Tunik, J. Jänis, M. Haukka, A. S. Melnikov, P. Y. Serdobintsev, T. A. Pakkanen, *Dalton Trans.*, 2010, **39**, 2676–2683.

View Article Online
DOI: 10.1039/C9NJ03426A